[Frontiers in Bioscience 12, 3781-3794, May 1, 2007]

Hepatic knockdown of stearoyl-COA desaturase 1 via RNA interference in obese mice decreases lipid content and changes fatty acid composition

Haiyan Xu, Denise Wilcox, Phong Nguyen, Martin Voorbach, Harriet Smith, Sevan Brodjian, Thomas Suhar, Regina M. Reilly, Peer B. Jacobson, Christine A. Collins, Katherine Landschulz, Terry K. Surowy

Metabolic Disease Research, Abbott Laboratories, Abbott Park, Illinois 60064

TABLE OF CONTENTS

1. ABSTRACT

Stearoyl-CoA desaturases (SCDs) catalyze the biosynthesis of monounsaturated fatty acids from saturated fatty acids. Four scd genes have been identified in mice and three in human (including one pseudogene). Among the four mouse SCD isoforms, SCD1 is predominantly expressed in liver and adipose tissue. Mice null for the scd1 gene have reduced adiposity, increased energy expenditure and altered lipid profiles. To further evaluate the specific role of hepatic SCD1 and the potential to achieve similar desirable phenotypic changes in adult obese mice, adenovirus-mediated short hairpin interfering RNA (shRNA) was used to acutely knock down hepatic scd1 expression in *ob/ob* mice. Robust reductions in hepatic SCD1 mRNA and SCD1 enzymatic activity were achieved, sustained up to 2 weeks. Reduced hepatic content of neutral lipids and robust lowering of lipid desaturation indexes, but increased content of liver phosphotidylcholine were observed with SCD1 knockdown. Increased total plasma cholesterol levels were also observed. No significant changes in body weight were observed. Expression levels of several lipogenic and lipid oxidation genes were not significantly altered by short term SCD1 reduction, but UCP2 expression was increased. Our results demonstrate that significant changes to both hepatic and systemic lipid profiles can be achieved through specific knockdown of liver-expressed SCD1 in the *ob/ob* mouse model. However, hepatic SCD1 knockdown does not result in significant changes in body weight in the short term.

2. INTRODUCTION

Obesity is characterized by massive expansion of fat mass and adipose tissue is the major site for long-term energy storage in the form of triacylglycerol (TAG). SCDs convert saturated fatty acids to monounsaturated fatty acids with stearic acid (18:0) as the most preferred substrate for most SCDs characterized (1). The SCDs also play an important role in TAG synthesis. The major fatty acid species in TAG is oleic acid (18:1), which is the main product of reactions catalyzed by SCDs. SCDs belong to the Δ^9-desaturase family, and are localized to the endoplasmic reticulum. The function of SCDs is to introduce a single double bond between carbons 9 and 10 in fatty acyl-CoAs that are either derived from the diet or are synthesized *de novo* (2). The activity of SCDs requires the presence of the reduced form of nicotinamide adenine dinucleotide and two other cofactors, cytochrome b5 and cytochrome b5 reductase (2, 3). In addition to their important role in TAG synthesis, SCDs are important for synthesis of cholesterol esters, wax esters and phospholipids, in which oleic acid is the predominant monounsaturated fatty acid (3).

Among the four scd genes identified in mice, scd 1 is mainly expressed in liver and adipose tissue; scd2 is expressed in neuronal tissues, including brain, and is important in lipid metabolism in early life (4, 5); scd3 is mainly detected in skin and Harderian gland (6) and scd4 is primarily expressed in heart (7). Only two SCD isoforms,

SCD1 and SCD5, as well as the existence of a pseudogene, have been reported in humans (8-11). Human SCD1 shows 85% identity to the murine SCD1 and is also similarly homologous to the other mouse SCD isoforms; in contrast human SCD5 shares approaching only 60% identity with mouse SCDs and with human SCD1. Distinct substrate specificities have been reported for murine SCDs: SCD1, SCD2 and SCD4 desaturate both stearic and palmitic acids while SCD3 only uses palmitic acid as the substrate (12). Among the four murine scd genes, scd1 has been most extensively characterized and has been demonstrated to play important roles in lipid metabolism and cholesterol homeostasis.

The expression of the scd1 gene is highly regulated by diet, hormones such as insulin and leptin, as well as by polyunsaturated fatty acids and cholesterol (13-21). SCD1 activity is upregulated several-fold in the liver of *ob/ob* mice and can be normalized by leptin treatment (22). Higher SCD1 activity in humans has been correlated with elevated plasma TAG levels (23). SCD1 expression is elevated in skeletal muscle of obese humans and overexpression of hSCD1 in myotubes from lean subjects was shown to lead to increased acetyl CoA carboxylase 2 (ACC2) activity and decreased fatty acid oxidation (24).

Absence of SCD1 activity, through a naturally existing mutation in the scd1 gene (asebia mice, ab^J/ ab^J) (25, 26) or through targeted disruption (1, 27), alters lipid metabolism, reduces adiposity and increases energy expenditure. Deficiency of SCD1 results in decreased levels of tissue TAGs, cholesterol esters and wax esters as well as significantly lowered TAG levels in plasma VLDL (26, 28), indicating that SCD1 plays an important role in TAG metabolism and secretion, and cholesterol homeostasis. Supplementation of oleate and palmitoleate in diet could not rescue the decrease in synthesis of TAGs and cholesterol esters caused by SCD1 deficiency, indicating a stringent requirement of monounsaturated fatty acids derived from *de novo* lipogenesis (26, 29). $Scd1^{-/-}$ mice also consume more food, but despite this, they clearly show a leaner phenotype when backcrossed to *ob/ob* mice or fed a high fat diet (22, 27). The lean phenotype can be explained by increased energy expenditure, which appears to be due to increased fatty acid oxidation through activation of AMP-activated kinase (30) and is independent of activation of the PPARα pathway (31). In adult diet-induced obese mice, lowered activity of SCD1 in liver and white and brown adipose tissue, achieved through delivery of SCD1-specific antisense oligonucleotides, also led to altered lipid metabolism and increased energy expenditure (32). Changes in lipid metabolism and reduced body weight gain were observed at 4 weeks, and decreased hepatic steatosis and increased energy expenditure were observed at 10 weeks.

In addition to altering lipid metabolism, deficiency or lowered SCD1 expression can affect glucose homeostasis and insulin signaling. SCD1 knockout mice have improved glucose tolerance, but similar fasting blood glucose levels to their wild-type counterparts (27). SCD1 knockout mice have lowered fasting insulin levels on a chow diet, but not on a high fat diet (27). Increased basal phosphorylation of the insulin receptor, insulin receptor substrate-1 and Akt were observed in muscle and brown adipose tissue of SCD1 knockout mice, accompanied by decreased mRNA, protein and activity of PTP1B, providing a basis for improved insulin sensitivity in these tissues (33, 34). In adult diet-induced obese mice, antisense oligonucleotide–mediated lowering of SCD1 activity was shown to lower postprandial plasma insulin and glucose levels, at 10 weeks into treatment, indicating improved systemic insulin sensitivity in this model (32). Recently, acute reduction of hepatic SCD1 activity in high-fat fed and insulin-resistant rats was achieved through SCD1 antisense oligonucleotide delivery and was accompanied by improved hepatic insulin sensitivity, but was associated with increased hepatic TAG content (35). The data suggest that SCD1 plays a critical role in the onset of diet-induced hepatic insulin resistance. Thus, SCD1 appears to play a role in insulin sensitivity, but mechanisms though which this is achieved, and the influence of diet, are still not fully elucidated

In order to further understand the role of hepatic versus adipose SCD1 and their respective contributions to altered lipid metabolism and obesity, tissue specific intervention of SCD1 activity will be necessary. In our study, through the application of RNA interference using adenovirus-mediated shRNA, we have achieved acute knock down of scd1 expression in livers of *ob/ob* mice, a model of obesity with significantly increased hepatic SCD1 expression and activity. Acute knockdown of SCD1 expression did not affect body weight or food intake, but significantly changed hepatic and systemic lipid profiles, and provided novel information on the role of hepatic SCD1 in lipid metabolism.

3. MATERIALS AND METHODS

3.1. Construction of adenovirus vectors for expressing shRNAs against mSCD1

In order to construct adenovirus vectors expressing shRNAs against mouse SCD1, five short hairpin oligonucleotides and complementary strands were designed to specifically target mouse SCD1. The BLOCK-iT™ RNAi system (Invitrogen, Carlsbad, CA) was used for shRNA construction. Briefly, the top and bottom oligonucleotides were annealed and ligated into the Gateway-based pENTR/U6 vector (Invitrogen, Carlsbad, CA) and sequence confirmed. To evaluate the potency of these shRNAs *in vitro*, the full-length mSCD1 cDNA was fused to EGFP cDNA in the pEGFP-N1 vector (BD biosciences, Mountain View, CA) so that it could be used in co-transfection with the entry plasmids expressing the SCD1 shRNAs. The co-transfection was performed in mouse L and HEK293A cells using Lipofectamine 2000 (Invitrogen, Carlsbad, CA), with 1μg of mSCD1-EGFP fusion plasmid and 5μg of pENTR/U6-shRNA plasmids. Cells were harvested forty-eight hours later for testing knock down efficiency. In order to generate the recombinant adenovirus vectors expressing shRNAs for mSCD1, selected pENTR/U6-shRNA plasmids were recombined into the Gateway-based pAd-BLOCK-iT

Table 1. Sequences of GFP-shRNA and effective mSCD1-shRNA2 and 5

Gene Name	5' – 3'
GFP-shRNA	
Forward	caccGAAGCAGCACGACTTCTTCttcaagaga GAAGAAGTCGTGCTGCTTC
Reverse	aaaaGAAGCAGCACGACTTCTTCtctcttgaa GAAGAAGTCGTGCTGCTTC
mSCD1-shRNA2	
Forward	caccGCGCATCTCTATGGATATCttcaagagaGATATCCATAGSAGATGCGC
Reverse	aaaaGCGCATCTCTATGGATATCtctcttgaaGATATCCATAGSAGATGCGC
mSCD1-shRNA5	
Forward	caccGAGATCTCCAGTTCTTACAttcaagagaTGTAAGAACTGGAGATCTC
Reverse	aaaaGAGATCTCCAGTTCTTACAtctcttgaaTGTAAGAACTGGAGATCTC

Linker and cloning sequences are in lower case

DEST™ vector (Invitrogen, Carlsbad, CA), according to the manufacturer's instructions. As a negative control, a recombinant adenovirus vector expressing a shRNA directed against GFP was generated. The sequences of GFP-shRNA and effective mSCD1-shRNA2 and 5 are shown in Table 1.

Amplification of recombinant adenovirus was performed according to the manufacturer's instructions (Invitrogen, Carlsbad, CA) using HEK 293A cells. Crude cell lysates were used to confirm knock down of endogenous mSCD1 in primary mouse hepatocytes prior to purification of recombinant adenoviruses. Large-scale amplification and purification of recombinant Ad-shRNA viruses were performed by Welgen, Inc. (Worcester, MA). Purified viruses were tested for confirmation of mSCD1 knockdown efficacy in primary mouse hepatocytes prior to *in vivo* studies. For virus infection, primary hepatocytes were seeded on 6-well plates at a density of $1x10^6$ cells/well and infected with adenovirus at a MOI of 50. Cells were harvested forty-eight hours post-infection for real-time PCR analysis.

3.2. Immunoblot analysis

To assay the efficacy of mSCD1-shRNAs, mouse L and human HEK293A cells co-transfected with plasmids expressing mSCD1-shRNAs and mSCD1-EGFP fusion protein were washed with ice-cold PBS forty-eight hours after transfection and lysed with CytoBuster™ protein extraction buffer (Novagen, San Diego, CA) supplemented with complete, EDTA-free protease inhibitor cocktail (Roche, Nutley, NJ). Sixty micrograms of cell lysate protein from each sample were used for immunoblot analysis according to the manufacturer's protocol (Invitrogen, Carlsbad, CA). Briefly, following SDS-PAGE, the resolved proteins were transferred onto PVDF membranes. Membranes were blocked in 5% non-fat dry milk in Tris-buffered saline containing 0.5% Tween 20 (TBST) for 1 hr, then incubated with a rabbit polyclonal antibody for GFP (Santa Cruz Biotechnology Inc., Santa Cruz, CA) at 1:100 dilution in 5% non-fat dry milk/ TBST. After four washings in TBST, membranes were incubated with a biotinylated goat anti-rabbit IgG (Kirkegaard & Perry Laboratories, Gaithersburg, Maryland) for 1hr at the dilution of 1:4000. Finally, streptavidin-labeled horseradish peroxidase (HRP, Kirkegaard & Perry Laboratories, Gaithersburg, Maryland) was used at 1:100 for 45 minutes to detect signal. Protein bands were detected by enhanced chemiluminescence (ECL) immunoblotting detection reagent (Amersham, Piscataway, NJ).

3.3. RNA isolation and quantitave RT-PCR analysis

RNA samples were extracted using the TRIZOL® reagent (Invitrogen, Carlsbad, CA). The gene expression profile of mSCD1, FAS, ACC1, ACC2, L-CPT1, VLCAD and UCP2 were measured using real-time PCR (TaqMan® analysis). The RT-PCR assay was performed in a 25µl reaction in 96-well clear plate using RT-PCR Thermoscript one-step system Invitrogen, Carlsbad, CA) on ABI Prism thermal cyclers model 7900 (Applied Biosystems, Framingham, MA). Reactions contained 1x reaction mix, 5.5 mM $MgSO_4$, 400 nM forward primer, 400 nM reverse primer and 100 nM probe (Applied Biosystems, Framingham, MA). The gene expression profile of mtGPAT1, DGAT1, DGAT2, PGC-1α, PEPCK, FBP1, and G6Pase were measured using cyber green real-time PCR analysis. Reactions contained 1x reaction mix, 5.5 mM $MgSO_4$, 300 nM forward primer and 300 nM reverse primer (Applied Biosystems, Framingham, MA). PCR conditions were: 50°C for 30 min followed by 95°C for 5 min for 1 cycle, and then 95°C for 15 sec followed by 60°C for 1 min for 40 cycles. The relative mRNA expression levels were normalized to expression of 28S rRNA. The sequences for the primer and probe sets for mouse mSCD1, FAS, ACC1, ACC2, L-CPT1, VLCAD and UCP2 are shown in Table 2.

3.4. Animal protocols and blood chemistries

The Abbott Institutional Animal Care and Use Committee approved all protocols involving rodents in advance and all studies were conducted in an Association for Assessment and Accreditation of Laboratory Animal Care-approved barrier facility. Male B6.V-Lep *ob/ob* mice were purchased from Jackson laboratories and received at 5-6 weeks of age. Mice were allowed access to food and water ad libitum. Mice were individually housed in micro-isolator cages for one week prior to the study for acclimation. The mice were culled into experimental groups with equal average levels of postprandial glucose (measured using Precision PCx-Abbott Laboratories, Abbott Park, IL) and body weight. Mice were injected, via lateral tail vein, with 150µl vehicle (PBS/10% glycerol, sterile and endotoxin-free) or adenovirus expressing either GFP-shRNA or mSCD1-shRNA. Five and fourteen days post injection, body weight and food intake were measured. Mice were euthanized at the end of studies under fed condition and blood was drawn by cardiac puncture and centrifuged for plasma collection. One third of each liver was snap frozen for mRNA and protein analysis. The second third was put into ice-cold buffer containing 250mM sucrose, 10mM Tris-Cl, pH 7.4, 1mM DTT and

Table 2. Sequences of the primer and probe sets for mouse mSCD1, FAS, ACC1, ACC2, L-CPT1, VLCAD, UCP2, mtGPAT1, DGAT1, DGAT2, PGC-1α, PEPCK, FBP1, and G6Pase

Gene Name	5' – 3'
mSCD1	5' – 3'
Forward	5' CCGAAGTCCACGCTCGAT
Reverse	5' GCCGGCATGATGATAGSTCAGT
Probe	P- 5' TCAGCACTGGGAAAGTGAGGCGAGC
FAS	
Forward	F- 5' ACCATGGAGCGTATATGTGAACA
Reverse	R- 5' CAATGCCCACGTCACCAA
Probe	P- 5' TGGCCTCCCAGGCCTTGCCGT
ACC1	
Forward	F- 5' ACCGCCAGCTTAAGGACA
Reverse	R- 5' TGGATGGGATGTGGGCA
Probe	P- 5' CACCTGTGTGGTGGAATTTCAGTTCATGC
ACC2	
Forward	F- 5' ACAGAGATTTCACCGTCGCGT
Reverse	R- 5' CGCAGCGATGCCATTGT
Probe	P- 5' ACTCGGTTTGGAGGCAACAGGGTCAT
L-CPT1	
Forward	ATCGTGAGTGGCGTCCTCTT
Reverse	CAGCGAGTAGCGCATAGTCATG
Probe	ACAGGGCTCTGGGTGGCGAT
VLCAD	
Forward	GCTGAGACGGAGGACAGGAAT
Reverse	ACCACGGTGGCAAATTGATC
Probe	AGAGCCTGCACTGCCAGTTCACCACT
UCP2	
Forward	CTGTTGATGTGGTCAAGACGAGAT
Reverse	CAGTGACCTGCGCTGTGGTA
Probe	CATGAACTCTGCCTTGGGCCA
mtGPAT1	
Forward	TCTGCTGCCATCTTTGTCCAC
Reverse	TTGGTCTCTTTGAAAACCCCG
DGAT1	
Forward	TGCTACGACGAGTTCTTGAG
Reverse	CTCTGCCACAGCATTGAGAC
DGAT2	
Forward	GCGCTACTTCCGAGACTACTT
Reverse	GGGCCTTATGCCAGGAAACT
PGC-1α	
Forward	TATGGAGTGACATAGAGTGTGCT
Reverse	CCACTTCAATCCACCCAGAAAG
PEPCK	
Forward	CTGCATAACGGTCTGGACTTC
Reverse	CAGCAACTGCCCGTACTCC
FBP1	
Forward	CACCGCGATCAAAGCCATCT
Reverse	AGGTAGCGTAGGACGACTTCA
G6Pase	
Forward	CGACTCGCTATCTCCAAGTGA
Reverse	GTTGAACCAGTCTCCGACCA

1 mM EDTA for isolation of microsomes. The remaining third of each liver was fixed in 10% formalin for histology. Plasma TAGs (Infinity kits, Thermo Electron Corporation, Louisville, CO), cholesterol (Infinity kits, Thermo Electron Corporation, Louisville, CO), and AST (Sigma Diagnostics, St. Louis, MO) were measured according to manufacturer's instructions.

3.5. Isolation of primary hepatocytes

Male B6 normal and B6.V-Lep *ob/ob* mice were anesthetized by intraperitoneal injection of ketamine (87mg/kg, Webster Veterinary Supply, Sterling, MA) and xylazine (13mg/kg, Webster Veterinary Supply, Sterling, MA). The peritoneal cavity was opened to expose the liver and portal vein. The portal vein was cannulated with a 24 gauge Abbocatheter (Abbott Hospital Supplies, North Chicago, IL) and stabilized with a bulldog clip. The cannula was then attached to a perfusion pump (Cole-Palmer Instrument Company, Vernon Hills, IL), and the Vena Cava was severed to allow drainage. The liver was perfused first with pre-warmed perfusion buffer (41°C) containing NaCl 8.7 g/L, Na-HEPES 2.4 g/L, D-fructose 3 g/L, EGTA 0.19 g/L, phenol red 10 mg/L and heparin 1000 U/L, for 4 minutes at the speed of 12ml /minute. Buffer was subsequently replaced with collagenase buffer containing KCl 0.5 g/L, NaCl 8.7g/L, Na-HEPES 2.4 g/L, $CaCl2{\cdot}2H_2O$ 0.74 g/L, D-fructose 3 g/L, phenol red 10 mg/L, 0.2% BSA, collagenase 100 U/ml (Sigma Chemicals, St. Louis, MO), hyaluronidase 47 U/ml (Sigma Chemicals, St. Louis, MO) and trypsin inhibitor 170 U/ml (Sigma Chemicals, St. Louis, MO) , and perfusion continued for approximately another 6 minutes until tissue was completely digested. The liver was then removed, rinsed in perfusion buffer, and mechanically macerated with a metal comb. The resulting cell suspension was then passed through a 105 micron nylon mesh sieve (Spectrum Laboratories, Rancho Dominguez, CA). Cells were washed twice in DMEM with 10% FBS and collected by centrifugation at 500x g for 3 minutes at 4°C. Cells were resuspended in plating medium, passed through 114 micron nylon mesh sieve, and seeded at a density of $1x10^6$/ well on 6-well plates. Cell viability was determined using trypan blue exclusion. Eighty-five percent viability was required for performing experiments.

3.6. Isolation of microsomes and SCD1 activity assay

Fresh liver samples from *ob/ob* mice were homogenized in a Dounce homogenizer in 6ml cold homogenization buffer (10mM Tris-HCl, pH7.4, 250mM sucrose, 1mM DTT, 5mM $MgCl_2$ and Complete proteinase inhibitor cocktail). After homogenization, the liver lysates were centrifuged at 10,000x g for 10 minutes to pellet large membranes including mitochondria. The supernatant was transferred to clean tubes and centrifuged at 100,000x g for 1 hr at 4°C. The pellet was resuspended with cold assay buffer (10mM Tris-Cl, pH 7.4, 5mM $MgCl_2$, 250mM sucrose, Complete-EDTA proteinase inhibitor cocktail, 1mM DTT and 50mM NaF) for protein quantification and enzymatic assay. SCD activities were assayed at 25°C for 1 hr with assay buffer supplemented with 2mM NADH, 10□M stearoyl-coenzyme A (Avanti Polar Lipids), 0.25μM [^{3}H] stearoyl-coenzyme A (American Radiolabeled Chemical, Inc, ART 390, 50-60 mCi/mmol) and 12.5μg of microsomal protein. The reaction was stopped by adding two volumes of ethanol. The mixture was loaded to charcoal filter plates pre-wet with methanol for capture of unused substrate and newly generated oleoyl-coenzyme A. The charcoal plates were centrifuged at 1000x g for 10 minutes to collect flow-through, which contains the other reaction product, $[^3H]H_2O$.

3.7. Lipid analysis

Approximately 100mg each of snap-frozen and pulverized liver samples were sent to Lipomics Technology Inc. for lipid profile analysis. In-house, liver TAG was measured using a method based on measurement of glycerol released from triglycerides. Briefly, approximately

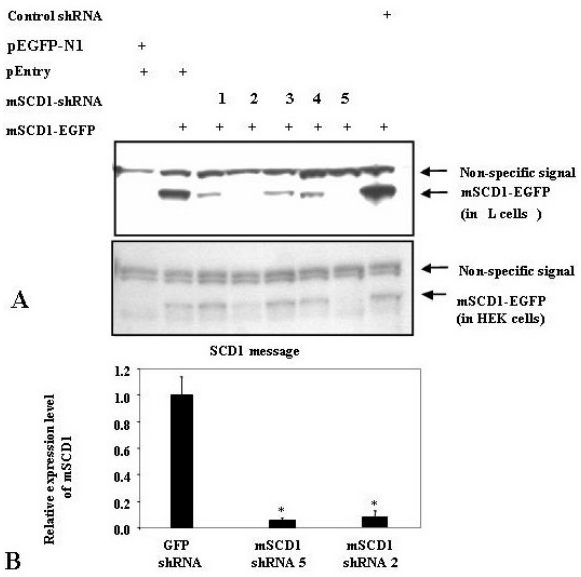

Figure 1. Selection of shRNAs against mSCD1 and knockdown in hepatocytes. 1A. Five short hairpin interfering RNAs (shRNA) against mSCD1 were designed and cloned into a Gateway-based entry vector containing the human U6 promoter. The entry vectors containing different hairpins were co-transfected with a vector expressing mSCD1-EGFP fusion protein into both L cells and HEK293A cells. Western analysis was performed to assess the expression level of mSCD1-EGFP using an antibody for GFP. 1B. SCD1-shRNAs 2 and 5 were selected and recombined into adenovirus vectors. Purified viruses containing mSCD1-shRNA 2 or 5 were used to infect primary hepatocytes isolated from *ob/ob* mice and knockdown effect was assessed by quantitative PCR analysis.

100 mg of liver tissue was homogenized in thirty volumes of ethanol using a Polytron homogenizer. Lipids were further extracted by vortexing homogenized samples for 15 minutes, cell debris was allowed to settle, and further clarification was achieved by centrifugation of the supernatant at 15,000x g for 10 minutes at room temperature. Assay of TAG was performed using a 96-well format. Samples were diluted 1:5 for assay. For standards, Lipid Lin-Trol standards were used (Sigma Chemicals, St. Louis, MO). For both standards and samples, 24 x volume of Infinity Triglyceride Reagent (Thermo Electron Corporation, Louisville, CO) was added and samples were incubated at 37°C for 5 min. After cooling down to room temperature, absorbance of samples was read at 520nm. Plasma triglyceride and cholesterol lipoprotein profiling was performed with a SMART fast protein liquid chromatography (FPLC) system (Pfizer, formerly Pharmacia) using a Superose 6 PC 3.2/30 column (Amersham Biosciences). 50 µl of pooled plasma sample was loaded onto the column. The elution flow rate was 40 µl /min in a running buffer consisting of 0.15 M NaCl and 0.05 M sodium phosphate pH 7.0. Fractions of 40 µl were collected and triglyceride and cholesterol contents were determined using enzymatic assay kits (Infinity, Thermo Electron Corporation). VLDL-cholesterol, LDL-cholesterol and HDL-cholesterol were quantified by a method that ensured that contributions from overlapping chromatographic peaks were correctly measured. The total cholesterol chromatographic profile was deconvoluted into three separate Gaussian peaks, one for each lipid type. These individual Gaussian curves were then fitted under constraints that required that their sum fit the entire chromatographic profile.

3.8. Statistical analysis

The student t-test was used to compare the difference between animals treated with adenovirus expressing shRNA against mSCD1 and shRNA against GFP.

4. RESULTS

4.1. Selection of shRNAs for knockdown of SCD1

Five shRNAs were designed to specifically target mouse SCD1 without affecting other SCD isoforms. Oligonucleotides representing the hairpin RNAs were cloned into pENTR/U6, a Gateway-based entry vector in which shRNA expression is driven by the human U6 promoter. The entry vectors containing different hairpins were co-transfected with a vector expressing mSCD1-EGFP fusion protein into both L cells and HEK293A cells. Forty-eight hours after transfection, immunoblot analysis was performed to examine the expression level of the fusion protein using an antibody against GFP (Figure 1A). The expression level of mSCD1-EGFP was reduced to an undetectable level when co-transfected with mSCD1-shRNAs 2 and 5 into L cells, and was barely detectable when co-transfected with the same two shRNAs into HEK293A cells. The remaining three shRNAs were not as effective for SCD1 knockdown. Mouse SCD1-shRNA2 and -shRNA5 were recombined into a Gateway system-based adenovirus destination vector. The efficacy of recombinant adenovirus expressing mSCD1-shRNA2 and shRNA5 were evaluated by infecting primary mouse hepatocytes from *ob/ob* mice with the viruses and assaying SCD1 mRNA levels using quantitative RT-PCR analysis. At a multiplicity of infection (MOI) of 50, both mSCD1-shRNA 5 and mSCD1-shRNA 2 potently reduced the expression level of endogenous mSCD1 by more than 90% (Figure 1B).

4.2. Hepatic SCD1 knockdown in *ob/ob* mice

In order to understand the importance of mSCD1 in liver glycerolipid and cholesterol ester synthesis, mSCD1-shRNA 5 was injected into *ob/ob* mice at $1x10^9$ pfu per mouse, and expression of SCD1 was evaluated at 5 and 14 days post injection using quantitative RT-PCR analysis. At the dose of $1x10^9$pfu /mouse, hepatic SCD1 mRNA was reduced by 58% five days post injection and by 83% fourteen days post injection, compared to control GFP-shRNA-injected mice (Figure 2A). Our results demonstrated that SCD1 knockdown by adenovirus-mediated shRNA was markedly effective even out to 14-days after injection. In fact, at 14 days, SCD1 mRNA expression was equivalent to that of control lean mice

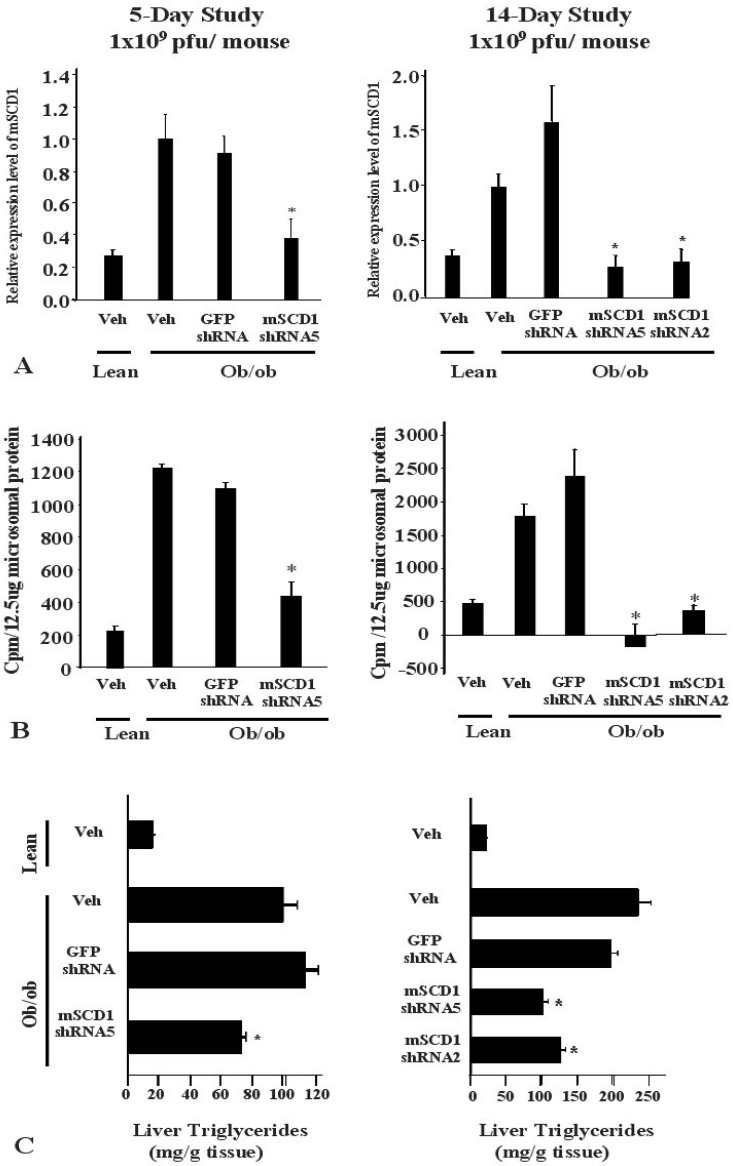

Figure 2. *In vivo* knock down of SCD1 in ob/ob mice. Adenovirus containing shRNA against GFP or mSCD1 was injected into *ob/ob* mice via tail vein at the dose of $1x10^9$ pfu /mouse. Saline was also injected at the same volume as vehicle control. Five and fourteen days post injection, mice were sacrificed and livers were taken. 2A. Expression levels of mSCD1mRNA in liver samples from lean mice treated with vehicle, and ob/ob mice treated with vehicle, adenovirus expressing GFP-shRNA or mSCD1-shRNAs. 2B. Activities of mSCD1 in liver samples from lean mice treated with vehicle, and ob/ob mice treated with vehicle, adenovirus expressing GFP-shRNA or mSCD1-shRNAs. 2C. Hepatic TAGs levels in lean mice treated with vehicle, and ob/ob mice treated with vehicle, adenovirus expressing GFP-shRNA or mSCD1-shRNAs. * Indicates $P<0.05$ for mSCD1 knockdown mice versus GFP-shRNA treated mice.

(Figure 2A, right panel). To increase our confidence of on-target specificity in knockdown, mSCD1-shRNA 2 was also injected into *ob/ob* mice at $1x10^9$ pfu/ mouse and expression of SCD1 was assessed 14 days post injection. SCD1 mRNA was reduced by 79% fourteen days post injection, relative to GFP shRNA-treated control mice, demonstrating that both SCD1 shRNAs are almost equally potent *in vivo* (Figure 2A, right panel). No reduction of liver mSCD1 mRNA was observed in mice treated with control GFP-shRNA compared to mice treated with vehicle. We also assayed SCD1 mRNA levels in white adipose tissue because of its abundant expression in this site. It is well-established that adenovirus does not get delivered to adipose tissue, and that it is predominantly delivered to liver. Using quantitative PCR analysis, we demonstrated that mSCD1 mRNA levels in white adipose tissue were unchanged after mSCD1 shRNA injection (data not shown). This information confirms that our data presented here represent the consequences of liver-specific SCD1 reduction by adenovirus-mediated shRNA delivery.

Even though our shRNAs were designed to be specific for mSCD1, SCD4 is also expressed at a very low level in mouse liver, so we assayed for its expression after delivery of SCD1 shRNAs. Quantitative PCR analysis demonstrated that SCD4 mRNA levels were not altered by treatment with either mSCD1-shRNA 2 or 5 (data not shown). To detect the consequences of SCD1 knockdown on SCD1 protein expression, we measured SCD1 enzymatic activity. Concomitant with knockdown of SCD1 mRNA, decreased SCD1 enzymatic activity was clearly observed, and was well-correlated with the extent of mRNA reduction. In *ob/ob* mice treated with mSCD1-shRNA 5, SCD1 enzymatic activity was reduced by 60% at five days post injection (Figure 2B, left panel) and knocked down to an undetectable level fourteen days post injection with delivery at the same dose (Figure 2B, right panel). Consistently, injection of mSCD1-shRNA2 at the same dose knocked down SCD1 enzymatic activity by 84% at fourteen days post injection, similar to SCD1 activity in lean mice treated with vehicle (Figure 2B, right panel). To evaluate the outcome of reduced SCD1 activity on hepatic lipid content, liver TAG levels were measured. TAG represents by far the most abundant lipid species in the liver. In *ob/ob* mice with steatotic livers, TAG levels are more than 10-fold higher than those of their lean counterparts. Compared to GFP-shRNA-treated *ob/ob* mice, liver TAG levels in mSCD1-shRNA 5 treated *ob/ob* mice were significantly reduced by 40% at five days post injection (Figure 2C, left panel) and decreased by 43% at fourteen days post injection (Figure 2C, right panel). This phenotype was confirmed with injection of mSCD1-shRNA 2, which reduced liver TAG levels by 28% at fourteen days post injection at the same dose (Figure 2C, right panel). Although substantially reduced, these TAG levels are nevertheless at least five-fold of those in the lean control mice (Figure 2C).

4.3. Effects of SCD1 knockdown on hepatic lipid content and composition

To investigate other changes in hepatic lipids that occurred with mSCD1 knock down, lipid profiling was performed with liver samples collected at fourteen days post injection from mSCD1-shRNA 5 and GFP-shRNA-treated *ob/ob* mice. In addition to reduction of TAGs, the level of hepatic diacylglycerols (DAGs) were significantly reduced by 22%, cholesterol esters (CEs) were decreased by 51%, and phosphotidylcholine (PC) increased by 45%, compared to levels in GFP-shRNA-treated mice (Figure 3A). The changes in hepatic CE and PC are consistent with the phenotypes reported with SCD1 knock out mice (26, 36), and the lowered DAG levels we observed provides novel information, at least in the *ob/ob* mouse model, for phenotype resulting from lowered hepatic SCD1 activity. The preferred substrates for SCD1 are palmitoyl-(16:0) and stearoyl- (18:0) CoAs. Reduction of SCD1 activity in livers of *ob/ob* mice mainly impacted the composition of these fatty acids in hepatic lipids, and of their Δ^9-desaturase products, palmitoleoyl (16:1n7) and oleoyl-(18:1n9) CoAs; oleoyl-CoA is the major monounsaturated fatty acid species in lipids (Figure 3B). In *ob/ob* mice treated with mSCD1-shRNA 5, the mole percentage (%) of 16:0 and 18:0 in TAG increased by 24% and 1000%, respectively, while those of 16:1n7 and 18:1n9–decreased by 54% and 55%, respectively, compared to control mice treated with GFP-shRNA. In DAGs, mole % of 16:0 and 18:0 increased by 24% and 231%, respectively, while the mole % of 16:1n7 and 18:1n9 decreased by 49% and 41%. Likewise, in CEs, the mole % of 16:0 and 18:0 increased by 74% and 272% respectively while the mole % of 18:1n9 decreased by 63%, and 16:1n7 trended downwards by 54%. The changes are fitting with lowered SCD1 activity. Most noticeable in the different neutral lipids are the dramatic increased mole %s of 18:0, the preferred substrate for SCD1. In phospholipids, there is also decreased mole % of the monounsaturated fatty acids 16:1n7 and 18:1n9, which occurred to approximately the same extent as seen for neutral lipids. For example, in PC, the mole % of 18:1n9 and 16:7n1 decreased by 50% and 52%, respectively; in phosphotidylethanolamine (PE) and cardiolipin (CL), the mole % of 18:1n9 was decreased by 50% and 43%, respectively (Figure 3B). In contrast, what distinguished phospholipid changes from neutral lipid changes, is the relatively mild increases seen for the preferred SCD1 substrates, 16:0 and 18:0, which in several phospholipids classes do not reach significance. For example, the 18:0 mole % trended upwards less than 10 % in PC and CL, and increased significantly by only 14 % in PE. The phospholipids are more heavily biased in their composition toward the saturated fatty acids. When we compared the changes in fatty acids on the basis of content (nmol/gram wet liver) rather than mole %, many of the relative changes seen were essentially similar. Thus, for example, decreased content of 18:1n9 was seen in TAG, DAG, and CE (to 25%, 46 % and 19 % of control values, respectively), in addition to decreased mole %. In addition, actual content of 18:0 increased in all of the neutral lipids, in addition to the mole %. For neutral lipids, changes in synthesis appeared to go hand in hand with changes in composition, suggesting that decreased monounsaturated fatty acid drives decreased synthesis. For phospholipids, the most apparent difference between evaluating data by mole % and actual content was seen in the PC fraction. Although mole % of saturated fatty acid was not significantly changed, actual content of 16:0 in PC was increased by 156% relative to control and for 18:0 the content increased by 164 %, whereas content of 16:1n7 and 18:1n9 decreased. Here, then, the increased total PC synthesis seen with SCD1 knockdown results in actual increased incorporation of saturated fatty acids, and decreased incorporation of major monounsaturated fatty acids.

Overall, the total mole % of saturated fatty acids (SFAs) is significantly increased in all neutral lipids examined: up by 93% in TAGs, 45% in DAGs and 61% in CEs (Figure 4A). The total mole % of monounsaturated fatty acids (MUFAs) is significantly reduced (primarily due to the decrease of n9 fatty acids): down by 52% in TAGs, 41% in DAGs and 58% in CEs. Similar changes in mole % of SFAs and MUFAs are also observed in some phospholipid species but to a lesser extent (Figure 4A). Interestingly, the mole % of polyunsaturated fatty acids (PUFAs) is also increased in most of the lipids profiled. The increase is mostly due to the increase of mole % of n6 fatty acids (Figure 4A). However, when we examined the

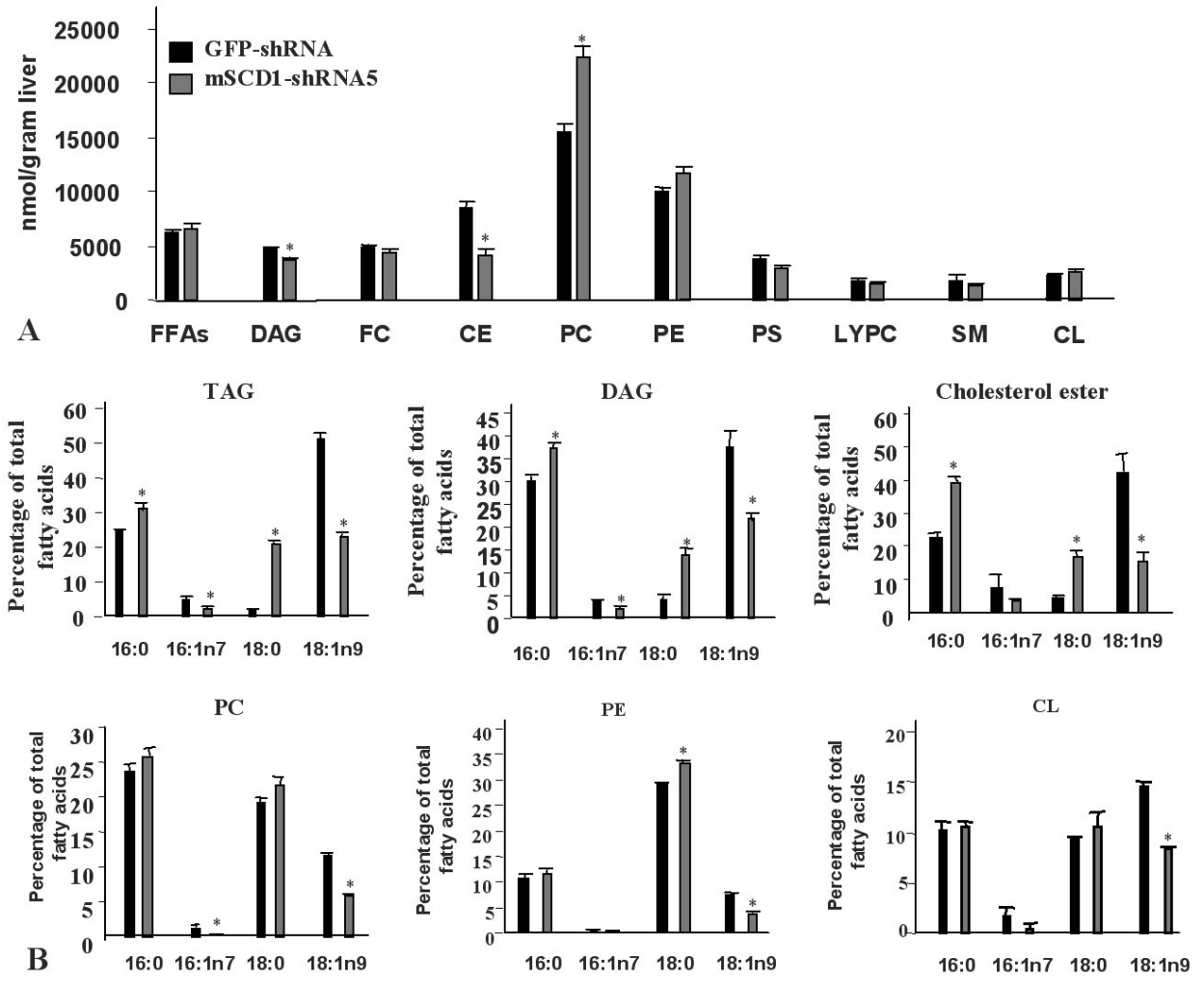

Figure 3. Lipid profiling of SCD1 knockdown livers from *ob/ob* mice. Liver samples were collected from *ob/ob* mice treated with adenovirus expressing GFP-shRNA or mSCD1-shRNA5 for fourteen days at the dose of $1x10^9$ pfu/mouse for lipid analysis. 3A. Hepatic contents of FFAs, DAGs, FC, CE, PC, PE, PS, LYPC, SM and CL. 3B. Fatty acid composition of 16:0, 16:1, 18:0, and 18:1 in hepatic TAGs, DAGs, CEs, PCs, PEs, and CLs. FFAs, free fatty acids; TAG, triacylglycerol; DAG, diacylglycerol; FC, free cholesterol; CE, cholesterol ester; PC, phosphotidylcholine; PE, phosphotidylethanolamine; PS, phosphatidylserine; LYPC, lysophosphatidylcholine; SM, sphingomyelin; CL, cardiolipin. Black bars represent mice treated with GFP-shRNA; grey bars represent mice treated with mSCD1-shRNA 5. * Indicates $P<0.05$ for mSCD1 knockdown mice versus GFP-shRNA treated mice.

actual content (nmol /gram wet liver) of these different lipid classes, in almost all lipid classes, including in all neutral lipids, only MUFAs and n9 fatty acid actually changed significantly, indicating that no compensatory changes in synthesis of SFA or PUFA incorporation occurred, as typified by TAG (Figure 4A). The only exception was PC, where decreased MUFA and n9 fatty acid content (down approximately 30%) was accompanied by increased incorporation of SFAs and PUFAs (both 159 % of control), including of both n3 and n6 PUFAs (Figure 4A).

Thus SCD1 knockdown in livers of *ob/ob* mice resulted in robust decreased mole % and actual content of MUFAs, particularly of 18:1n9, in neutral lipid species, accompanied by decreased overall neutral lipid synthesis. This was accompanied by increased mole% of SFAs and PUFAs, but without increased actual content of these fatty acids. For phospholipids, SCD1 knockdown resulted in less robust changes in mole % of fatty acids, but there was significant increased synthesis of PC. Increased PC synthesis was accompanied by increased incorporation of SFAs and PUFAs in addition to decreased incorporation of MUFAs; for other phospholipids, content changes were restricted to lowered MUFA incorporation.

A biomarker of SCD1 activity is the desaturation index (DI), defined as the ratio of 18:1/18:0 or 16:1/16:0.

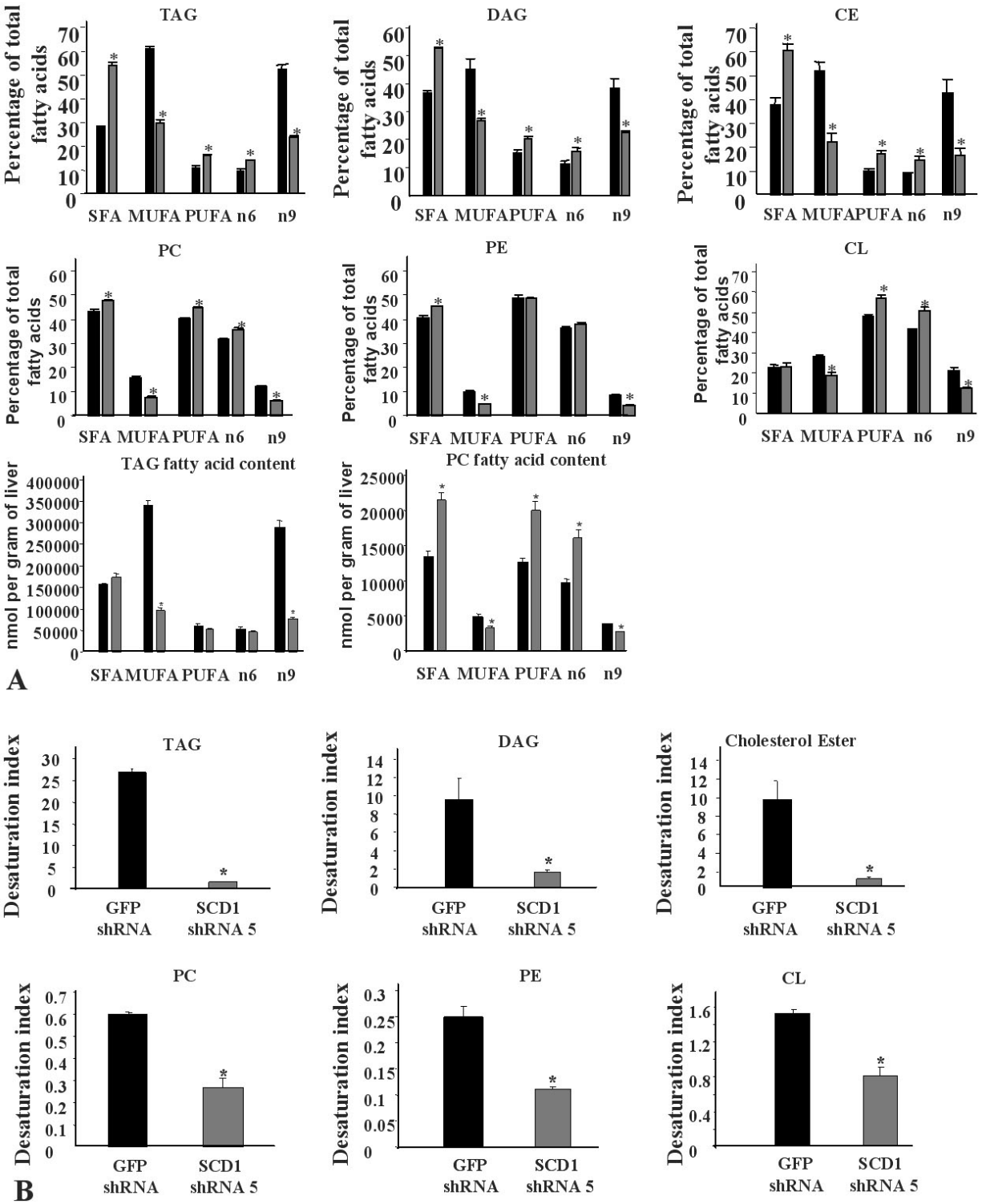

Figure 4. Changes of lipid desaturation in SCD1 knockdown livers from *ob/ob* mice**.** Liver samples were collected from *ob/ob* mice treated with adenovirus expressing GFP-shRNA or mSCD1-shRNA5 for fourteen days at the dose of $1x10^9$ pfu/mouse for fatty acid composition by classes in neutral and phospholipids. 4A. Fatty acid composition by percentage of total fatty acids in TAG, DAG, CE, PC, PE, and CL; and by actual content (nmol/ gram wet liver) in TAGs and PC. Black bars represent mice treated with GFP-shRNA; grey bars represent mice treated with mSCD1-shRNA 5. 4B. Desaturation index in hepatic TAG, DAG, CE, PC, PE, and CL in SCD1 knockdown livers compared to control livers. * Indicates $P<0.05$ for mSCD1 knockdown mice versus GFP-shRNA treated control mice.

Table 3. Measurement of metabolic parameters in SCD1 knock down and control mice

		TAG (mg/dL)	Cholesterol (mg/dL)	Weight (g)	FI (g)	AST (mg/dL)	VLDL-TAG (mg/dL)	HDL-Cholesterol (mg/dL)	LDL-Cholesterol (mg/dL)	VLDL-Cholesterol (mg/dL)
$1x10^9$ pfu 5-day	Vehicle	235.3±44	197.9±20	41.5 ±0.7	37.6 ±1.3	144.8±13	41	118	100	15
	GFP-shRNA	212.8±72	199.4±27	42.6 ±1.2	39.2 ±1.9	168.5± 8	38	115	100	17
	mSCD1-shRNA5	209.4±41	257±20[1]	41.3 ±0.7	36.1 ±2.3	175.6±17	91	115	160	25
$1x10^9$ pfu 14-day	Vehicle	145.8±20	258 ±21	56.6 ±1.3	92.8 ±5.2	184.5±37	19	123	90	8
	GFP-shRNA	95.8 ±6.5	212 ±16	55.2 ±1.3	73.0 ±3.3	260.7±58	14	90	90	10
	mSCD1-shRNA5	122±10.7	345 ±17[1]	53.3 ±1.3	76.5 ±4.9	284.3±38	31	105	163	13
	mSCD1-shTNA2	116 ±6	350 ±12[1]	52.8 ±0.9	83.8 ±7.5	282.9±28	37	114	145	11

Six to thirteen mice were used for each analysis. Values are presented as means ± standard errors, except for plasma lipoprotein analysis results, for which pooled plasma samples from all mice in an experimental group were used and a single value is reported for each lipoprotein type. [1] Means $P<0.05$ for mSCD1 knockdown mice versus GFP-shRNA treated mice. FI, accumulative food intake over the entire experimental period

It is not only associated with obesity but is also implicated in the regulation of cell growth and differentiation through effects on membrane fluidity and signal transduction (37). When we expressed changes in lipid composition in SCD1 knockdown *ob/ob* mice as the 18:1/18:0 desaturation index (DI), it was clear that DI was dramatically reduced in hepatic neutral lipids: down by 96% in TAGs, 83% in DAGs, and 90% in cholesterol esters (Figure 4B). Of all lipid parameters determined, DI most clearly showed the effect of SCD1 knockdown on neutral lipid composition. In contrast, the reduction of desaturation index is modest, but still significant, in several phospholipids (Figure 4B), probably because monounsaturated fatty acids are generally much less represented. The changes in the ratios of 16:1/16:0 were similar to those observed with 18:1/18:0 (data not shown).

4.4. Metabolic profiling of SCD1 knockdown *ob/ob* mice

In addition to changes in lipid content and composition in liver, plasma lipid parameters were also evaluated in SCD1 knockdown *ob/ob* mice. In the 5-day study, total plasma cholesterol levels were significantly increased by 29% in SCD1 knockdown *ob/ob* mice compared to control mice treated with GFP-shRNA (Table 3). Increased total plasma cholesterol has been reported in SCD1 knock out mice, so these data demonstrate that similar effects of lowered SCD1 activity are borne out in adult obese mice. Our results also suggest that alteration of hepatic SCD1 activity is sufficient to change total plasma cholesterol. In the 14-day study, both mSCD1-shRNA5 and mSCD1-shRNA2 were used to treat *ob/ob* mice. Plasma cholesterol levels were significantly increased by 63% and 65%, respectively, in SCD1 knockdown mice compared to control *ob/ob* mice treated with GFP-shRNA. When plasma lipoproteins were fractionated by size exclusion chromatography and cholesterol were quantified in the different lipoprotein fractions, it was clear that the increased plasma cholesterol resulting from SCD1 knockdown was predominantly due to increased LDL-cholesterol (Table 3). A 60% increase over controls was observed on day 5 in the 5-day study with mSCD1-shRNA5. 81% and 61% increases for animals treated with mSCD1-shRNA5 and mSCD1-shRNA2, respectively, were observed at end of 14-day study. Although present at much lower levels, VLDL-cholesterol was also increased with SCD1 knockdown in both studies to a lesser extent (Table 3). In contrast to changes of total plasma cholesterol, no significant change was observed in total plasma TAGs with SCD1 knockdown (Table 3). Nevertheless, with size fractionation of plasma lipoproteins and assay of TAGs in each faction, it was evident that VLDL-TAG was increased with SCD1 knockdown, compared to ob/ob mice treated with GFP-shRNA. In the 5-day study, a 2.4-fold increase was observed at day 5, and consistent with this, 2.2-fold and 2.6-fold increases were seen for mSCD1-shRNA5 and mSCD1-shRNA2, respectively, at end of the 14-day study (Table 3). Since the TAG assay is based on glycerol quantification, free glycerol present in rodent plasma contributes significantly to quantification of total TAG. In contrast to the changes in plasma lipoproteins observed with knockdown of liver SCD1, no changes in body weight or food intake were observed. Liver function was assayed by examining plasma levels of AST. Levels of this enzyme did not change significantly in adenovirus-treated mice compared to vehicle-treated control mice (Table 3).

4.5. Hepatic gene profiling

In order to understand whether hepatic lipogenesis and/or fatty acid oxidation were affected by reduction of SCD1 activity in livers of *ob/ob* mice, expression of selected genes involved in lipid synthesis and fatty acid oxidation were evaluated by real-time PCR analysis with liver samples from all studies in which mSCD1-shRNA5 or GFP-shRNA was injected (Table 4). Genes involved in *de novo* lipogenesis include fatty acid synthase (FAS), acetyl CoA carboxylase 1 (ACC1) and 2 (ACC2); genes involved in triglyceride synthesis include mitochondrial glycerol-3-phosphate acyltransferase 1 (mtGPAT1), diacylglycerol acyltransferase 1 (DGAT1) and 2 (DGAT2); genes involved in fatty acid oxidation include carnitine palmitoyl transferase 1a (CPT-1a), very long chain acyl CoA dehydrogenase (VLCAD) and uncoupling protein 2

Table 4. Expression of genes involved in lipid and glucose metabolism in liver of SCD1 knock down *ob/ob* mice

Gene	5-Day Study ($1x10^9$ pfu/mouse)		14-Day study $1x10^9$ pfu/mouse	
	GFP-shRNA	SCD1-shRNA5	GFP-shRNA	SCD1-shRNA5
SCD1	100 ± 33	13 ± 4.2[1]	100 ± 9.5	7 ± 2.5[1]
FAS	100 ± 13	112 ± 27	100 ± 27	101 ± 15
ACC1	100 ± 20	114 ± 8.2	100 ± 23	74 ± 6
ACC2	100 ± 1	116 ± 12	100 ± 15	77 ± 5.4
mtGPAT1	100 ± 15.4	197 ± 29.8[1]	100 ± 10.2	96 ± 17.1
DGAT1	100 ± 37.1	133 ± 12.2	100 ± 15	115 ± 31.1
DGAT2	100 ± 17.5	185 ± 30.1[1]	100 ± 10.9	91 ± 19.5
L-CPT1	100 ± 11	128 ± 5.2	100 ± 4.7	97 ± 7.7
VLCAD	100 ± 4	100 ± 5.4	100 ± 22	62 ± 4.7
UCP2	100 ± 24	141 ± 9.1[1]	100 ± 5	138 ± 14.2[1]
PGC-1alpha	100 ± 11.7	102 ± 10.6	100 ±16.3	85 ± 18.1
PEPCK	100 ± 8.2	94 ± 13.1	100 ± 31.3	84 ± 11
FBP1	100 ± 7.4	137 ± 20.5	100 ± 4.8	115 ± 11
G6Pase	100 ±11.8	193 ± 36.2[1]	100 ± 21.5	165 ± 14.1[1]

Five to ten mice were used for individual RNA preparation within each group. The expression level of each gene in SCD1 knock down mice is presented as percentage of the expression level of the same gene in GFP-shRNA treated mice. [1] indicates statistical significance with $P<0.05$

(UCP2). The expression levels of FAS, ACC1, and ACC2 were not significantly changed in the 5-day and 14-day studies, suggesting that *de novo* lipogenic pathway was not affected at the level of gene regulation. Surprisingly, despite decreased TAG synthesis, there was an almost 2-fold increase of mtGPAT1 and DGAT2 mRNA 5 days post virus injection, which returned to baseline 14 days post virus injection. The expression level of DGAT1 did not have significant change. Among the three oxidative genes examined, the expression level of UCP2 significantly increased in all studies, up by 41% in the 5-day study, and increased by 38% in the 14-day study. The expression levels of CPT-1a (liver isoform) and VLCAD, however, did not change in these studies. In addition to lipid metabolism, decreased SCD1 expression using an anti-sense approach has been reported to reduce hepatic glucose production. Therefore, genes involved in glucose metabolism, including PGC-1alpha, PEPCK, FBP1, and G6Pase, were also examined. The expression levels of PGC-1alpha, PEPCK, and FBP1 did not change significantly. However, expression level of G6Pase significantly increased in both studies, up to almost 2-fold at day 5 in the 5-day study, and increased 60% at the end of the 14-day study.

5. DISCUSSION

As a rate-limiting enzyme in synthesis of monounsaturated fatty acids, SCD1 has now been shown to be an important player in promoting obesity and insulin resistance (38). Highly expressed in liver and adipose tissue, which are tissues important for lipid metabolism, SCD1 is also the major isoform of Δ^9 desaturase in these tissues. Liver is an organ critical in regulating transient energy fluctuations. It is not only capable of regulating lipid synthesis through the *de novo* lipogenic pathway but also plays a key role in clearing diet-derived lipids and transporting excessive TAGs to adipose tissue for storage via VLDL secretion.

In this study, we evaluated the effect of lowered hepatic SCD1 activity on hepatic and circulating lipid metabolism in *ob/ob* mice by specifically knocking down SCD1 expression in liver using RNA interference via an adenovirus-mediated shRNA approach, without affecting SCD1 expression in adipose tissue. Using two different shRNAs specific for SCD1 we were able to demonstrate that SCD1 RNA interference was effective at reducing SCD1 mRNA levels and enzyme activities in livers of *ob/ob* mice, whereas no such changes were observed in GFP-shRNA-treated mice compared to mice injected with vehicle. Consistency of response was seen with both shRNAs, supporting on-target knockdown. With SCD1 shRNA-5 that was delivered for both 5 and 14 days, it was evident that the longer 14-day duration of shRNA knockdown resulted in further reduced SCD1 expression and enzyme activity comparable to those observed in lean mice.

In these short-term studies, we observed robustly decreased hepatic neutral lipid content, in TAGs, DAGs and CEs, down 40-50%, and dramatically lowered desaturation index in these lipids, down 83-96%. Desaturation index changes clearly indicate the extent of on-target effects of SCD1 knockdown. Fatty acid composition analysis revealed that the most dramatic changes were increased mole % of 18:0 and reduced mole % of 18:1 in neutral lipids, followed by similar changes in composition of 16:0 and 16:1. This is consistent with literature that 18:0 is the most preferred substrate for SCD1. The decreased content of stored TAGs and cholesterol esters indicates that supply of long chain monounsaturated fatty acyl-CoAs, especially oleoyl-CoA, is a major regulator promoting their synthesis in the liver. The results are consistent with those observed in SCD1 knock out mice (26). In addition, they inform us that even in the grossly obese adult *ob/ob* mouse, with TAG levels 10-20 fold of lean mice, it is possible to have dramatic effects on liver lipid content and composition through robust lowering of hepatic SCD1 activity. Lowered liver total lipid desaturation index and reduced steatosis have been reported for SCD1 knockdown through antisense oligonucleotide delivery in diet-induced obese mice, which reduced SCD1 expression in both liver and fat (32). Our results demonstrate that liver-specific knockdown of SCD1 is sufficient to drive dramatic changes in liver lipid content and composition. Our study also provided the novel observation of decreased hepatic DAGs associated with SCD1 knockdown in obese mice, which was not observed with SCD1 knock out in lean mice (36). It suggests that hepatic content of this lipid can also be regulated by the supply of monounsaturated fatty acyl-CoAs. Increased levels of hepatic DAGs have been associated with liver insulin resistance, possibly through DAG-mediated activation of hepatic protein kinase C_ε (11, 39). Therefore, decreased DAG levels seen with lowered SCD1 activity in the *ob/ob* model might have beneficial effects toward reversal of hepatic insulin resistance. Through

measurement of actual content of liver neutral lipids, we demonstrated that despite reduced incorporation of monounsaturated fatty acid into TAGs, DAGS, and CEs upon SCD1 knockdown, there are no compensatory increases in incorporation of SFAs or PUFAs into these lipid classes.

In addition to decreased liver TAG, DAG and CE content, we found that SCD1 knockdown resulted in increased hepatic PC content by 45%. The increased PC content is in agreement with similarly increased PC synthesis reported in SCD1 knockout mice (36). Phosphatidylcholine is a primary phospholipid in cellular membranes, plasma lipoproteins and bile, and is key to proper liver function. In addition, it serves as an important second messenger in signal transduction. There are two pathways of PC synthesis, one utilizing CDP-choline and DAG (the Kennedy pathway) and the other utilizing phosphatidylethanolamine. The former is responsible for synthesizing approximately 70% of hepatic PC, while the latter provides PC to VLDL and bile (36). In SCD1 knockout mice, it has been demonstrated that deficiency of SCD1 leads to activation of CTP:choline cytidyltransferase translocation, the enzyme which catalyzes the synthesis of CDP choline, presumably due to altered membrane composition (36). The increased CDP-choline formation then leads to enhanced hepatic PC synthesis. This may also explain the increased PC synthesis that we observed. Since DAG is also required for PC synthesis, increased PC synthesis may contribute to decreased hepatic DAG content. Despite the fact that SCD1 did not affect the absolute levels of other phospholipids, desaturation indexes were significantly reduced in all phospholipid classes, although to a much lesser extent compared to those in neutral lipids, supporting previous indications that SCD1 plays a bigger role in providing substrates for synthesis of neutral lipids. As with neutral lipids, lowered desaturation index in phospholipids was not, in general, associated with compensatory increases in PUFA and SFA incorporation, except for PC.

It is interesting to observe that liver specific knockdown of SCD1 in *ob/ob* mice resulted in increased plasma cholesterol (predominantly LDL-cholesterol) and plasma VLDL-TAG within the 14-day duration of the study. Effects on liver CE and TAG synthesis, content and composition may be expected to alter plasma lipoprotein profiles through effects on lipid secretion. It is important to note here that SCD1 activity has also been reported to modulate membrane domain structure and to inhibit / destabilize ATP-binding cassette transporter A-1 (ABCA1)-mediated cholesterol efflux (11, 40). ABCA1 facilitates cholesterol and phospholipid efflux from liver and macrophages to extracellular lipid-poor apolipoproteins, initiating the formation of HDL. Passive transfer of cholesterol and phospholipids to extracellular acceptors such as LDL and HDL is also known to occur. Alterations, as a result of SCD1 knockdown, in one or more of the processes mentioned above may explain the increased plasma LDL and VLDL-cholesterol we observed in SCD1 knockdown *ob/ob* mice. Further studies are required to investigate our observations.

Although changes in lipid profiles were seen with liver-specific knockdown of SCD1, some features observed in SCD1 knockout mice, such as decreased body weight and increased food intake, were not observed in our *ob/ob* mice with relatively short-term liver-specific SCD1 knock down. Likewise, recently-reported short-term (4-day) knockdown of SCD1 in liver and fat of rats (35) did not result in loss of body weight nor increase of food intake. In another SCD1 antisense oligonucleotide study, performed in diet-induced obese mice (32), food intake was not altered with knockdown of SCD1 in liver and fat, but decrease in weight gain was observed 4 weeks after treatment, and continued to the end of study at 10 weeks. Lack of effect on body weight observed in our study could be due to shorter study duration, although it is possible that liver-specific SCD1 knockdown is not sufficient. Regarding food intake, our results and those of others suggest that ablation of SCD1 activity developmentally may result in a different phenotype than intervention of SCD1 function pharmacologically in adult rodents. It is possible that SCD1 function in brain might be important for regulating food intake, which is a tissue not accessible to antisense oligonucleotides nor adenovirus delivered systemically.

At 14-days post SCD1 shRNA delivery, and with robust liver-specific knockdown of SCD1 in *ob/ob* mice, hepatic gene profiling revealed unchanged expression of several genes involved in lipogenesis and fatty acid oxidation, except for UCP2 and G6Pase in both 5-day and 14-day studies, and mtGPAT1 as well as DGAT2 in the 5-day study. The increased UCP2 expression suggests some uncoupling of respiration and potential increase in energy dissipation as heat in livers of the SCD1 knock down *ob/ob* mice. The exact role of UCP2 in liver is not yet fully understood, but it is thought to have control over energy status, possibly in the adaptation of lipid metabolism to excessive supply of fatty acids, in regulation of ketogenesis and in management of redox potential (41, 42). Increased expression of UCP2 in brown adipose tissue, a tissue well-known to be thermogenic, has been reported as a result of SCD1 knockdown in DIO mice using antisense oligonucelotide delivery (32). Our results are the first to demonstrate that increased UCP2 expression can also occur in liver as a result of SCD1 knockdown specifically in this tissue; they support interpretation that hepatic SCD1 exerts control over energy expenditure in liver. The apparent short-term increased mtGPAT1 and DGAT2 expression in *ob/ob* mice in response to knockdown of SCD1 in liver, together with the increased expression of G6Pase, could represent compensatory changes to rapid and robust reduction in hepatic lipid synthesis.

In summary, our data demonstrate that acute intervention of SCD1 activity in liver was sufficient to improve the hepatic lipid profile in obese mice, and exert gene expression changes indicating potential increased energy expenditure, but not enough to induce reduction of body weight. Although it is important to interfere with SCD1 activity in multiple tissues in order to achieve the beneficial effects of increased systemic energy expenditure, pharmacological intervention with small molecule drugs is often directed predominantly to liver. Our studies specifically targeting liver SCD1 provide insight into the

relatively short-term effects of hepatic SCD1 knockdown in *ob/ob* mice, a common rodent model of obesity.

6. ACKNOWLEDGEMENTS

We gratefully acknowledge Dr. Thomas H. Lubben for deconvolution of areas under the chromatographed plasma lipoprotein cholesterol peaks, enabling accurate quantification. Current address of Haiyan Xu: Brown Medical School, Hallett Center for Diabetes and Endocrinology, Providence, RI 02903

7. REFERENCES

1. Miyazaki, M., W. C. Man & J. M. Ntambi: Targeted disruption of stearoyl-CoA desaturase1 gene in mice causes atrophy of sebaceous and meibomian glands and depletion of wax esters in the eyelid. *J Nutr*, 131, 2260-8 (2001)
2. Miyazaki, M. & J. M. Ntambi: Role of stearoyl-coenzyme A desaturase in lipid metabolism. *Prostaglandins Leukot Essent Fatty Acids*, 68, 113-21 (2003)
3. Dobrzyn, A. & J. M. Ntambi: The role of stearoyl-CoA desaturase in body weight regulation. *Trends Cardiovasc Med*, 14, 77-81 (2004)
4. Kaestner, K. H., J. M. Ntambi, T. J. Kelly, Jr. & M. D. Lane: Differentiation-induced gene expression in 3T3-L1 preadipocytes. A second differentially expressed gene encoding stearoyl-CoA desaturase. *J Biol Chem*, 264, 14755-61 (1989)
5. Miyazaki, M., A. Dobrzyn, P. M. Elias & J. M. Ntambi: Stearoyl-CoA desaturase-2 gene expression is required for lipid synthesis during early skin and liver development. *Proc Natl Acad Sci U S A*, 102, 12501-6 (2005)
6. Zheng, Y., S. M. Prouty, A. Harmon, J. P. Sundberg, K. S. Stenn & S. Parimoo: Scd3--a novel gene of the stearoyl-CoA desaturase family with restricted expression in skin. *Genomics*, 71, 182-91 (2001)
7. Miyazaki, M., M. J. Jacobson, W. C. Man, P. Cohen, E. Asilmaz, J. M. Friedman & J. M. Ntambi: Identification and characterization of murine SCD4, a novel heart-specific stearoyl-CoA desaturase isoform regulated by leptin and dietary factors. *J Biol Chem*, 278, 33904-11 (2003)
8. Zhang, S., Y. Yang & Y. Shi: Characterization of human SCD2, an oligomeric desaturase with improved stability and enzyme activity by cross-linking in intact cells. *Biochem J*, 388, 135-42 (2005)
9. Zhang, L., L. Ge, S. Parimoo, K. Stenn & S. M. Prouty: Human stearoyl-CoA desaturase: alternative transcripts generated from a single gene by usage of tandem polyadenylation sites. *Biochem J*, 340 (Pt 1), 255-64 (1999)
10. Beiraghi, S., M. Zhou, C. B. Talmadge, N. Went-Sumegi, J. R. Davis, D. Huang, H. Saal, T. A. Seemayer & J. Sumegi: Identification and characterization of a novel gene disrupted by a pericentric inversion inv (4) (p13.1q21.1) in a family with cleft lip. *Gene*, 309, 11-21 (2003)
11. Yu, C., Y. Chen, G. W. Cline, D. Zhang, H. Zong, Y. Wang, R. Bergeron, J. K. Kim, S. W. Cushman, G. J. Cooney, B. Atcheson, M. F. White, E. W. Kraegen & G. I. Shulman: Mechanism by which fatty acids inhibit insulin activation of insulin receptor substrate-1 (IRS-1)-associated phosphatidylinositol 3-kinase activity in muscle. *J Biol Chem*, 277, 50230-6 (2002)
12. Miyazaki, M., S. M. Bruggink & J. M. Ntambi: Identification of mouse palmitoyl-coenzyme A Delta9-desaturase. *J Lipid Res*, 47, 700-4 (2006)
13. Hu, C. C., K. Qing & Y. Chen: Diet-induced changes in stearoyl-CoA desaturase 1 expression in obesity-prone and -resistant mice. *Obes Res*, 12, 1264-70 (2004)
14. Miyazaki, M., A. Dobrzyn, W. C. Man, K. Chu, H. Sampath, H. J. Kim & J. M. Ntambi: Stearoyl-CoA desaturase 1 gene expression is necessary for fructose-mediated induction of lipogenic gene expression by sterol regulatory element-binding protein-1c-dependent and -independent mechanisms. *J Biol Chem*, 279, 25164-71 (2004)
15. Legrand, P., D. Catheline, J. M. Hannetel & P. Lemarchal: Stearoyl-CoA desaturase activity in primary culture of chicken hepatocytes. Influence of insulin, glucocorticoid, fatty acids and cordycepin. *Int J Biochem*, 26, 777-85 (1994)
16. Waters, K. M. & J. M. Ntambi: Insulin and dietary fructose induce stearoyl-CoA desaturase 1 gene expression of diabetic mice. *J Biol Chem*, 269, 27773-7 (1994)
17. Liang, C. P. & A. R. Tall: Transcriptional profiling reveals global defects in energy metabolism, lipoprotein, and bile acid synthesis and transport with reversal by leptin treatment in *ob/ob* mouse liver. *J Biol Chem*, 276, 49066-76 (2001)
18. Lee, K. N., M. W. Pariza & J. M. Ntambi: Conjugated linoleic acid decreases hepatic stearoyl-CoA desaturase mRNA expression. *Biochem Biophys Res Commun*, 248, 817-21 (1998)
19. Bene, H., D. Lasky & J. M. Ntambi: Cloning and characterization of the human stearoyl-CoA desaturase gene promoter: transcriptional activation by sterol regulatory element binding protein and repression by polyunsaturated fatty acids and cholesterol. *Biochem Biophys Res Commun*, 284, 1194-8 (2001)
20. Asilmaz, E., P. Cohen, M. Miyazaki, P. Dobrzyn, K. Ueki, G. Fayzikhodjaeva, A. A. Soukas, C. R. Kahn, J. M. Ntambi, N. D. Socci & J. M. Friedman: Site and mechanism of leptin action in a rodent form of congenital lipodystrophy. *J Clin Invest*, 113, 414-24 (2004)
21. Kim, H. J., M. Miyazaki & J. M. Ntambi: Dietary cholesterol opposes PUFA-mediated repression of the stearoyl-CoA desaturase-1 gene by SREBP-1 independent mechanism. *J Lipid Res*, 43, 1750-7 (2002)
22. Cohen, P., M. Miyazaki, N. D. Socci, A. Hagge-Greenberg, W. Liedtke, A. A. Soukas, R. Sharma, L. C. Hudgins, J. M. Ntambi & J. M. Friedman: Role for stearoyl-CoA desaturase-1 in leptin-mediated weight loss. *Science*, 297, 240-3 (2002)
23. Attie, A. D., R. M. Krauss, M. P. Gray-Keller, A. Brownlie, M. Miyazaki, J. J. Kastelein, A. J. Lusis, A. F. Stalenhoef, J. P. Stoehr, M. R. Hayden & J. M. Ntambi: Relationship between stearoyl-CoA desaturase activity and plasma triglycerides in human and mouse hypertriglyceridemia. *J Lipid Res*, 43, 1899-907 (2002)
24. Hulver, M. W., J. R. Berggren, M. J. Carper, M. Miyazaki, J. M. Ntambi, E. P. Hoffman, J. P. Thyfault, R.

Stevens, G. L. Dohm, J. A. Houmard & D. M. Muoio: Elevated stearoyl-CoA desaturase-1 expression in skeletal muscle contributes to abnormal fatty acid partitioning in obese humans. *Cell Metab*, 2, 251-61 (2005)
25. Zheng, Y., K. J. Eilertsen, L. Ge, L. Zhang, J. P. Sundberg, S. M. Prouty, K. S. Stenn & S. Parimoo: Scd1 is expressed in sebaceous glands and is disrupted in the asebia mouse. *Nat Genet*, 23, 268-70 (1999)
26. Miyazaki, M., Y. C. Kim, M. P. Gray-Keller, A. D. Attie & J. M. Ntambi: The biosynthesis of hepatic cholesterol esters and triglycerides is impaired in mice with a disruption of the gene for stearoyl-CoA desaturase 1. *J Biol Chem*, 275, 30132-8 (2000)
27. Ntambi, J. M., M. Miyazaki, J. P. Stoehr, H. Lan, C. M. Kendziorski, B. S. Yandell, Y. Song, P. Cohen, J. M. Friedman & A. D. Attie: Loss of stearoyl-CoA desaturase-1 function protects mice against adiposity. *Proc Natl Acad Sci U S A*, 99, 11482-6 (2002)
28. Miyazaki, M., H. J. Kim, W. C. Man & J. M. Ntambi: Oleoyl-CoA is the major de novo product of stearoyl-CoA desaturase 1 gene isoform and substrate for the biosynthesis of the Harderian gland 1-alkyl-2,3-diacylglycerol. *J Biol Chem*, 276, 39455-61 (2001)
29. Miyazaki, M., Y. C. Kim & J. M. Ntambi: A lipogenic diet in mice with a disruption of the stearoyl-CoA desaturase 1 gene reveals a stringent requirement of endogenous monounsaturated fatty acids for triglyceride synthesis. *J Lipid Res*, 42, 1018-24 (2001)
30. Dobrzyn, P., A. Dobrzyn, M. Miyazaki, P. Cohen, E. Asilmaz, D. G. Hardie, J. M. Friedman & J. M. Ntambi: Stearoyl-CoA desaturase 1 deficiency increases fatty acid oxidation by activating AMP-activated protein kinase in liver. *Proc Natl Acad Sci U S A*, 101, 6409-14 (2004)
31. Miyazaki, M., A. Dobrzyn, H. Sampath, S. H. Lee, W. C. Man, K. Chu, J. M. Peters, F. J. Gonzalez & J. M. Ntambi: Reduced adiposity and liver steatosis by stearoyl-CoA desaturase deficiency are independent of peroxisome proliferator-activated receptor-alpha. *J Biol Chem*, 279, 35017-24 (2004)
32. Jiang, G., Z. Li, F. Liu, K. Ellsworth, Q. Dallas-Yang, M. Wu, J. Ronan, C. Esau, C. Murphy, D. Szalkowski, R. Bergeron, T. Doebber & B. B. Zhang: Prevention of obesity in mice by antisense oligonucleotide inhibitors of stearoyl-CoA desaturase-1. *J Clin Invest*, 115, 1030-8 (2005)
33. Rahman, S. M., A. Dobrzyn, P. Dobrzyn, S. H. Lee, M. Miyazaki & J. M. Ntambi: Stearoyl-CoA desaturase 1 deficiency elevates insulin-signaling components and down-regulates protein-tyrosine phosphatase 1B in muscle. *Proc Natl Acad Sci U S A*, 100, 11110-5 (2003)
34. Rahman, S. M., A. Dobrzyn, S. H. Lee, P. Dobrzyn, M. Miyazaki & J. M. Ntambi: Stearoyl-CoA desaturase 1 deficiency increases insulin signaling and glycogen accumulation in brown adipose tissue. *Am J Physiol Endocrinol Metab*, 288, E381-7 (2005)
35. Gutierrez-Juarez, R., A. Pocai, C. Mulas, H. Ono, S. Bhanot, B. P. Monia & L. Rossetti: Critical role of stearoyl-CoA desaturase-1 (SCD1) in the onset of diet-induced hepatic insulin resistance. *J Clin Invest*, 116, 1686-95 (2006)
36. Dobrzyn, A., P. Dobrzyn, M. Miyazaki, H. Sampath, K. Chu & J. M. Ntambi: Stearoyl-CoA desaturase 1 deficiency increases CTP:choline cytidylyltransferase translocation into the membrane and enhances phosphatidylcholine synthesis in liver. *J Biol Chem*, 280, 23356-62 (2005)
37. Ntambi, J. M.: Regulation of stearoyl-CoA desaturase by polyunsaturated fatty acids and cholesterol. *J Lipid Res*, 40, 1549-58 (1999)
38. Dobrzyn, A. & J. M. Ntambi: The role of stearoyl-CoA desaturase in the control of metabolism. *Prostaglandins Leukot Essent Fatty Acids*, 73, 35-41 (2005)
39. Neschen, S., K. Morino, L. E. Hammond, D. Zhang, Z. X. Liu, A. J. Romanelli, G. W. Cline, R. L. Pongratz, X. M. Zhang, C. S. Choi, R. A. Coleman & G. I. Shulman: Prevention of hepatic steatosis and hepatic insulin resistance in mitochondrial acyl-CoA:glycerol-sn-3-phosphate acyltransferase 1 knockout mice. *Cell Metab*, 2, 55-65 (2005)
40. Sun, Y., M. Hao, Y. Luo, C. P. Liang, D. L. Silver, C. Cheng, F. R. Maxfield & A. R. Tall: Stearoyl-CoA desaturase inhibits ATP-binding cassette transporter A1-mediated cholesterol efflux and modulates membrane domain structure. *J Biol Chem*, 278, 5813-20 (2003)
41. Ricquier, D. & F. Bouillaud: Mitochondrial uncoupling proteins: from mitochondria to the regulation of energy balance. *J Physiol*, 529 Pt 1, 3-10 (2000)
42. Grav, H. J., K. J. Tronstad, O. A. Gudbrandsen, K. Berge, K. E. Fladmark, T. C. Martinsen, H. Waldum, H. Wergedahl & R. K. Berge: Changed energy state and increased mitochondrial beta-oxidation rate in liver of rats associated with lowered proton electrochemical potential and stimulated uncoupling protein 2 (UCP-2) expression: evidence for peroxisome proliferator-activated receptor-alpha independent induction of UCP-2 expression. *J Biol Chem*, 278, 30525-33 (2003)

Key Words: SCD1, RNA interference, Obesity, *ob/ob*

Send correspondence to: Dr. Haiyan Xu, Brown Medical School, Hallett Center for Diabetes and Endocrinology, 55 Claverick St., Rm 318, Providence, RI 02903, Tel: 401-444-0347, Fax: 401-444-3784, E-mail: hxu@lifespan.org

http://www.bioscience.org/current/vol12.htm